RESEARCH ARTICLE

Progress and challenges in advanced ground-based gravitational-wave detectors

M. Adier · F. Aguilar · T. Akutsu · M. A. Arain · M. Ando · L. Anghinolfi ·
P. Antonini · Y. Aso · B. W. Barr · L. Barsotti · M. G. Beker · A. S. Bell ·
L. Bellon · A. Bertolini · C. Blair · M. R. Blom · C. Bogan · C. Bond · F. S.
Bortoli · D. Brown · B. C. Buchler · H. J. Bulten · G. Cagnoli · M. Canepa ·
L. Carbone · E. Cesarini · B. Champagnon · D. Chen · A. Chincarini · A.
Chtanov · S. S. Y. Chua · G. Ciani · E. Coccia · A. Conte · M. Cortese ·
M. Daloisio · M. Damjanic · R. A. Day · D. De Ligny · J. Degallaix · M.
Doets · V. Dolique · K. Dooley · S. Dwyer · M. Evans · M. Factourovich · V.
Fafone · S. Farinon · D. Feldbaum · R. Flaminio · D. Forest · C. Frajuca ·
M. Frede · A. Freise · T. Fricke · D. Friedrich · P. Fritschel · V. V. Frolov ·
P. Fulda · M. Geitner · G. Gemme · J. Gleason · S. Goßler · N. Gordon ·
C. Gräf · M. Granata · S. Gras · M. Gross · H. Grote · R. Gustafson · M.
Hanke · M. Heintze · E. Hennes · S. Hild · S. H. Huttner · K. Ishidoshiro ·
K. Izumi · K. Kawabe · S. Kawamura · F. Kawazoe · M. Kasprzack · A.
Khalaidovski · N. Kimura · S. Koike · T. Kume · A. Kumeta · K. Kuroda ·
P. Kwee · B. Lagrange · P. K. Lam · M. Landry · S. Leavey · M. Leonardi ·
T. Li · Z. Liu · M. Lorenzini · G. Losurdo · D. Lumaca · J. Macarthur ·
N. S. Magalhaes · E. Majorana · V. Malvezzi · V. Mangano · G. Mansell ·
J. Marque · R. Martin · D. Martynov · N. Mavalvala · D. E. McClelland ·
G. D. Meadors · T. Meier · A. Mermet · C. Michel · Y. Minenkov · C. M.
Mow-Lowry · L. Mudadu · C. L. Mueller · G. Mueller · F. Mul · D. Nanda
Kumar · I. Nardecchia · L. Naticchioni · M. Neri · Y. Niwa · M. Ohashi · K.
Okada · P. Oppermann · L. Pinard · J. Poeld · M. Prato · G. A. Prodi · O.
Puncken · P. Puppo · V. Quetschke · D. H. Reitze · P. Risson · A. Rocchi · N.
Saito · Y. Saito · Y. Sakakibara · B. Sassolas · A. Schimmel · R. Schnabel ·
R. M. S. Schofield · E. Schreiber · V. Sequino · E. Serra · D. A. Shaddock ·
A. Shoda · D. H. Shoemaker · K. Shibata · D. Sigg · N. Smith-Lefebvre · K.
Somiya · B. Sorazu · M. S. Stefszky · K. A. Strain · N. Straniero · T. Suzuki ·
R. Takahashi · D. B. Tanner · G. Tellez · T. Theeg · C. Tokoku · K. Tsubono ·
T. Uchiyama · S. Ueda · H. Vahlbruch · G. Vajente · C. Vorvick · J. F. J. van
den Brand · A. Wade · R. Ward · P. Wessels · L. Williams · B. Willke · L.
Winkelmann · K. Yamamoto · J.-P. Zendri

In the print and PDF versions of this article the full author affiliation list is given at the end of the paper.

This article belongs to the Topical Collection: The First Century of General Relativity: GR20/Amaldi10.

D. H. Shoemaker (✉)
Massachusetts Institute of Technology, NW 22-295, 185 Albany Street, Cambridge, MA, USA
e-mail: dhs@mit.edu

Abstract The Amaldi 10 Parallel Session C3 on Advanced Gravitational Wave detectors gave an overview of the status and several specific challenges and solutions relevant to the instruments planned for a mid-decade start of observation. Invited overview talks for the Virgo, LIGO, and KAGRA instruments were complemented by more detailed discussions in presentations and posters of some instrument features and designs.

1 Introduction (S. Kawamura, D. Shoemaker)

In parallel with the building, commissioning, and observation with the initial generation of interferometric gravitational-wave detectors, a second generation of detectors was being enabled through laboratory-scale research and development. By the year 2000, the outlines of designs and sensitivity objectives were known, and detailed designs and proposals to funding agencies led to well-defined projects underway by 2010. This session covered the status of these second-generation instruments, with a planned $\sim 10\times$ improvement in sensitivity over the first generation of detectors. If actual rates of neutron-star inspirals are in the mid-band of our rate estimates, these instruments should see gravitational-wave signals roughly monthly, with first detections as early as 2016.

2 Status of advanced LIGO (Presenter: L. Barsotti on behalf of the LIGO Scientific Collaboration)

Two 4 km-long Advanced LIGO detectors are currently in their installation phase in United States, one in Hanford (WA) and one in Livingston (LA). The Livingston idetector, L1, is currently commissioning the central part of the interferometer, with all the main components integrated and tested, except the kilometric arms. A complementary strategy has been carried out on the Hanford interferometer, H1, where one of the two 4 km arms has been fully commissioned. Both interferometers are on target to complete the installation and to be operational in 2014, and to start collecting observational data in 2015. Compared to initisal LIGO, the high frequency performance (above a few hundred hertz) will be improved by increasing the amount of laser light power circulating inside the interferometers, the mid-band through reduction of thermal noise, while the low frequency part of the spectrum will approach the design target by reducing the impact of technical noises, such as seismic, and length and angular control noises.

Figure 1 shows a plausible progression, due to commissioning activities interleaved with observation, of Advanced LIGO sensitivity curves for the upcoming years.
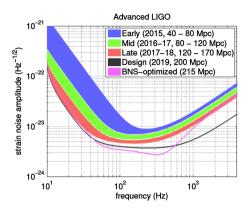
A third Advanced LIGO detector is planned to be located in India, thus improving the ability of the world-wide network to localize astrophysical sources, significantly increasing the network's scientific value.

3 Advanced Virgo (Presenter: G. Losurdo, for the Virgo Collaboration)

The Virgo interferometric detector of gravitational waves [2] is currently being upgraded to a "second generation" machine: Advanced Virgo. Together with Advanced

Fig. 1 Plausible progression of
aLIGO sensitivity curves over
the next decade [1]

LIGO, Geo HF and Kagra, Advanced Virgo will be part of the 2nd generation network aiming to open the way to gravitational wave astronomy. Advanced Virgo has participation by scientists from France and Italy, the initial founders of Virgo, as well as The Netherlands, Hungary and Poland. Its funding was approved in December 2009.

The construction of Advanced Virgo is progressing and, as of Nov 2013 more that 50 % of the investment budget has been spent. The main infrastructure works needed in the experimental halls have been completed and the installation of the equipment has started. In the forthcoming months the injection system will be completely installed and the commissioning of the input mode cleaner will start in mid 2014. The end of the assembly and integration phase is expected on July 2015, but before that date several elements of the detector will have been commissioned.

The overall construction strategy has been conceived in order to join the network as fast as possible; Fig. 2 shows a plausible progression of sensitivity. To this end Advanced Virgo will start its operation in a simplified configuration: the signal recycling mirror and the high power laser will not be installed in the early phase. This choice will likely reduce the commissioning time needed to reach a sensitivity good enough to contribute to the network and participate in an observing run in 2016.
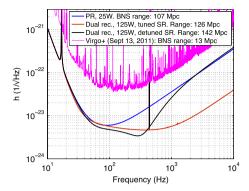
4 Progress and challenges of KAGRA (Presenter: S. Kawamura for the KAGRA collaboration)

KAGRA is the Large-scale Cryogenic Gravitational wave Telescope, hosted by Institute for Cosmic Ray Research, the University of Tokyo with strong support from the High Energy Accelerator Research Organization and National Astronomical Observatory of Japan, as well as from around 40 domestic and around 40 international institutes/universities. The objectives of KAGRA are to detect gravitational waves and to establish a new astronomy, gravitational wave astronomy, together with advanced LIGO, Advanced Virgo, and GEO-HF in the context of the worldwide network.

KAGRA consists of a 3km Resonant Sideband Extraction (RSE) interferometer with the cryogenic mirrors suspended from the Seismic Attenuation System (SAS).

Fig. 2 The sensitivity reached by Virgo (*magenta*) is compared with the target sensitivity of Advanced Virgo in various configurations: the *blue curve* is the target sensitivity of the initial configuration, with 25 W of laser power in the interferometer and no signal recycling. The corresponding inspiral range for binary neutron stars is 107 Mpc. The *red/black curves* are the target sensitivities of the dual recycled detector with 125 W of laser power, with tuned/detuned signal recycling cavity respectively. The inspiral range for binary neutron star coalescence for each configuration is indicated in the legend (color figure online)

The detector will be built underground in the Kamioka mine for significantly lower seismic noise. The mirrors of the arm cavities are cooled down to 20 K in order to reduce the thermal noise. For this purpose, sapphire substrates and fibers will be used because of the material's excellent mechanical and thermal properties. The RSE configuration allows us to optimize the quantum noise for the chirp signal expected from binary neutron star coalescences. The inspiral range for binary neutron star coalescences, corresponding to the sensitivity limit of KAGRA, is 176 Mpc.

After the tunnel excavation is completed, which is expected to happen in March of 2014, we plan to build KAGRA in two stages: initial KAGRA (iKAGRA) and baseline KAGRA (bKAGRA). iKAGRA is a simple Fabry-Perot Michelson interferometer with a modest vibration isolation system and fused silica test masses at room temperature. We decided to start with iKAGRA to gain some useful experience for a km-class interferometer and also to learn technical challenges for bKAGRA. We plan to conduct a short observation run at the end of 2015. Then we will proceed to bKAGRA, which is an RSE interferometer with a full SAS and sapphire mirrors at cryogenic temperature. We hope to finish the installation and commissioning of bKAGRA and then to start observation runs around 2017–2018.

The current status of KAGRA is as follows: The beam tubes and cryostats have been already manufactured and delivered. Various cryogenic and mechanical characterization of the cryogenic system has been performed. Two sapphire mirrors have been delivered and the optical parameters of the sapphire piece have been measured. A part of the SAS prototype has been tested and characterized. However, still most challenging is the development of the cryogenic suspension system for bKA-GRA.

KAGRA employs an underground location and cryogenic mirrors, which are key technologies for the 3rd-generation gravitational wave detectors, such as the Einstein Telescope. Therefore, KAGRA also plays an important role for future generations to further develop gravitational wave astronomy.

5 GEO-HF commissioning update (Presenter: K. Dooley)

The German-British laser interferometer gravitational-wave detector, GEO 600 is located near Hannover, Germany. It has served as the sole interferometric gravitational-wave detector in operation since September 2011. While other observatories worldwide are being upgraded and constructed, GEO 600 has been collecting science quality data with a duty cycle of approximately 2/3. The data will be searched for gravitational waves in the event of an external trigger indicating, for example, a supernova in our Galaxy. Data quality tools aid our monitoring of the detector [13]. GEO 600 is expected to run together with early Advanced detectors, as they come online over the next few years. Above about 1 kHz, the potential target sensitivity of GEO 600 is similar to that of the early Virgo detector (in Virgo's foreseen first phase without Signal recycling mirror).

In parallel to its data-taking mode, GEO 600 is implementing a series of upgrades intended to improve its strain sensitivity at high frequencies (above 500 Hz) [14]. Called GEO-HF, this program involves the application of squeezing, and addressing technical challenges of increasing the circulating laser power from about 2 to 20 kW. Commissioning is underway. Since the start of the GEO-HF program in 2009, a factor of 4 improvement in strain sensitivity at 4 kHz has been achieved.

Recent squeezing work includes developing new phase and alignment signals to actively control the squeezed vacuum field with respect to the interferometer. We also demonstrated a squeezing duty cycle of 90 % over 11 months yielding an average 26 % improvement in sensitivity at 4 kHz [15].

Recent developments towards increasing the laser power include the design and use of a thermal compensation system. The installation of side heaters on one of the end mirrors has corrected an astigmatism, reducing the power of higher order modes at the dark port by 37 % and demonstrating the success of segmented thermal compensation [16].

6 New in-air seismic attenuation system for gravitational wave detectors (Presenter: M.R. Blom)
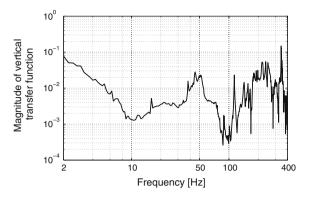
To eliminate the external injection bench (EIB) as a source of beam jitter that would limit the sensitivity of Advanced Virgo [4] we developed a seismic attenuation system to isolate the EIB from ground vibrations, called EIB-SAS. It employs vertical and horizontal anti-spring filters and a real-time digital control system to attenuate seismic noise by 40 dB above 10 Hz. A full description of our system can be found in Ref. [5]. We reported the seismic attenuation performance in the vertical direction. The vertical transfer function is shown in Fig. 3. Transfer functions in the other degrees of freedom have been measured, but will be reported elsewhere.

The vertical transfer function of EIB-SAS decreases with f^{-2} up to 10 Hz as expected. The resonances have been identified and damped as needed. In its current state, EIB-SAS meets the seismic attenuation requirement in the vertical direction by a large margin.

7 Development of the coatings for the Advanced LIGO and Advanced Virgo mirrors (Presenter: R. Flaminio)

Mirror parameters such as surface flatness, coating absorption or coating mechanical losses play a crucial role in the sensitivity of advanced gravitational wave detectors. The coatings for the cavity mirrors of Advanced LIGO (aLIGO) and Advanced Virgo (AdV) are being realized by the Laboratoire des Matériaux Avancés (LMA) in a 10m^3 ion beam sputtering chamber originally developed for the Virgo mirrors.

In order to have mirrors with surface figure error below 0.5 nm rms the coating thickness uniformity has to be a few parts in 10^4 over a diameter of 150 mm. The first set of mirrors for aLIGO was done in a configuration where the substrate undergoes a simple rotational motion in the chamber during the coating deposition, leading to a mirror flatness was about 0.8–0.9 nm rms for the end mirrors. The second set of mirrors was done in a configuration where the substrate undergoes a double rotation motion (so-called 'planetary motion') and two mirrors are coated at the same time. In this case the mirror flatness was reduced to about 0.7 nm rms for the end mirrors. The two mirrors being done at the same time, their figures are very similar. According to the simulation with these mirrors the round trip losses in the aLIGO arm cavities should be around 20 ppm. Simulation indicates that the interferometer contrast defect is expected to be about 10^{-4}).

Coating mechanical losses are measured at LMA by comparing mechanical losses of 110 μm thick silica cantilevers before and after coating deposition. Measurements made on coating monolayers shows that the losses of SiO$_2$ are around 5×10^{-5} and those of titania doped tantala are around 2.4×10^{-4}. According to the theory, the losses of coating multilayers should be a linear combination of the losses measured on the monolayers. Measurements made at LMA on coating multilayers deposited on thin cantilevers (either in silica or silicon) have shown a systemic excess of losses in the multilayers. The excess gets larger as the thickness of the multilayers increases and it was a factor of two in the case of cantilevers coated with coatings equal to those deposited on the aLIGO end mirrors. New measurements have been done with a 3-in. diameter 0.1 thick silica disc coated with a multilayer coating equal to the ones used for the aLIGO input mirrors, as well as a 3-in. diameter, 450 μm thick silicon disc. In

both cases the mechanical loss measurements give values much closer to the expected value. The expected and measured values are the same within the errors and the excess if any is smaller than 25 %.

8 Progress on the cryogenic system for the interferometric cryogenic gravitational wave telescope, KAGRA (Presenter: N. Kimura)
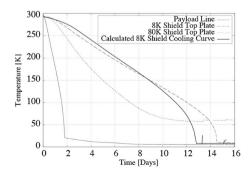
The Japanese large-scale cryogenic gravitational wave telescope, KAGRA, aims to detect gravitational waves using an interferometer having 3 km in length of arms. A notable feature of KAGRA is that the four main mirrors of the interferometer are cooled down below 20 K in order to reduce thermal noise. With the design of the cryogenic system for KAGRA, a cryo-payload consisting of the mirror and its suspension system is connected with two very-low-vibration cryo-cooler units as cooling devices, and is surrounded by the radiation shield (2.5 m^3 in volume) below 20 K in a cryostat. Each cooling device consists of a pulse-tube type cryocooler (0.9 W at 4 K), a specifically designed mechanical frame, and conduction cooling links made of 5N8 aluminum.

Fabrication of four cryostats and sixteen very-low-vibration cryocooler units was started at 2011, and completed on the end of March 2013. All of the cryocooler units confirmed their expected cooling performance, of 2.5 W at 9 K, and the overall vibration characteristic less than 10^{-7} m/$\sqrt{\text{Hz}}$ at the connection edge of conductive cooling passage. KAGRA collaborators carried out total performance tests including cooling characteristic with a half size of dummy cryo-payload and measurements of vibration of the radiation shield. Figure 4 shows typical cooling characteristics of the KAGRA cryostat.

9 Stabilized high power lasers for second and third generation gravitational wave detectors (Presenter: B. Willke)

Laser-interferometric Gravitational Wave Detectors (GWDs) require high power laser sources which operate at a single frequency and in a pure spatial mode with extraordinary stability in their temporal and spatial performance. Such a laser system for the Advanced LIGO (aLIGO) GWD with an optical power of 200 W was developed and stabilized by a collaboration of the Laser Zentrum Hannover and the Albert-Einstein-

Fig. 4 Typical cooling curves obtained from the cooling performance test of the cryostat

Institute (AEI) in Hannover, Germany [6,7] with three of these lasers installed. The spatial purity of these lasers can be quantified by the fractional power in higher order spatial modes (HOM); before filtering, 3.1, 5.3, and 8.5 % was observed and after spatial filtering with a so-called pre-mode-cleaner (PMC) less than 0.5 % was seen for all three systems. The fluctuations of the beam propagation direction were attenuated by the PMC to below $5 \, \text{nm}/\sqrt{\text{Hz}}$ and $5 \, \text{nrad}/\sqrt{\text{Hz}}$, respectively, for frequencies above 10 Hz. Temporal filtering of the laser beam by the pre-mode-cleaner provides a reduction of the laser power noise at radio frequencies. Using the optical AC-coupling measurement method we saw power fluctuations at the heterodyne sensing frequencies of aLIGO well below $10^{-9}/\sqrt{\text{Hz}}$ [8]. The stabilized power noise in the GWD detection frequency band above 10 Hz is less than $5 \times 10^{-8}/\sqrt{\text{Hz}}$ and will be further reduced by a second loop. The laser and the stabilization loops are computer controlled and acquire their relevant operation points in a fully automated way. Furthermore a diagnostic system [9] is an integral part of the laser system that allows to automatically measure the spatial as well as the temporal beam parameters of the laser.

Third generation GWDs laser sources might differ from the ones currently in use by their power, wavelength and spatial profile. We were able to demonstrate a highly stable 130 W laser at an operation wavelength of 532 nm [10] and an 82 W laser beam at 1,064 nm with a Laguerre Gauss LG_{33} spatial profile and with 95 % mode purity [11]. We have successfully started to employ fiber based technologies to fabricate lasers of up to 300 W output power [12] and are currently starting a measurement campaign to test their long term behavior, controllability and reliability.

10 Characterization of the input optics for the Advanced LIGO detectors (Presenter: C. L. Mueller)

The Advanced LIGO input optics are now being commissioned; they are tasked with stabilizing and preparing the laser beam before injection into the main interferometer. A trio of RF sidebands must be added to the beam, the frequency and pointing of the laser must be stabilized, and a Faraday Isolator must provide 30 dB of optical isolation from the interferometer reflected light. All of this must happen while operating at CW powers of 150 W and maintaining a 75 % throughput efficiency.

The electro-optic modulator uses rubidium titanyl phosphate (RTP) as the interaction medium. Modulation depths up to 0.4 are attainable with a residual amplitude modulation ratio of $AM/PM < 1 \cdot 10^{-4}$. The input mode cleaner (IMC) is responsible for pointing and frequency stabilization of the beam. It is a triangular resonant cavity with mirrors hanging from triple stage suspensions. Modeling indicates that the frequency noise out of the IMC will be within requirements, reaching $0.1 \text{Hz}/\sqrt{\text{Hz}}$ at 10 Hz and $1 \text{mHz}/\sqrt{\text{Hz}}$ at 100 Hz. The pointing noise into the IMC was found to be too high, but the source was identified as a noisy piezo actuated steering mirror. Noise budgeting indicates that the pointing noise will reach a level of $2 \text{nrad}/\sqrt{\text{Hz}}$ at 10 Hz once this issue is fixed, as required.

The in-vacuum Faraday isolator uses terbium gallium garnet (TGG) as the interaction medium. It uses calcite wedge polarizers for their high extinction ratio and is specially designed to partially compensate for both thermal lensing and thermal depo-

larization in the TGG crystal. Measurements show that the isolation ratio at 10 W is 43 dB and the isolation ratio stays above 34 dB up to 70 W of input power. Thermal lensing measurements indicate that the decrease in mode matching overlap due to thermal lensing will be ∼3.3 % at the full Advanced LIGO input power of 120 W.

11 Quantum noise reduction using squeezed states in LIGO (Presenter: S. Dwyer)

Squeezed states have the potential to improve the sensitivity of advanced gravitational wave detectors, and could provide an alternative route to achieving the design sensitivity of Advanced LIGO. We report on a demonstration of squeezing injection in an Enhanced LIGO detector, resulting in the best sensitivity demonstrated to date in a gravitational wave detector from 300 Hz up [36]. This experiment allowed us to investigate the technical risks of squeezing injection in a full scale gravitational wave detector [37] and the limits to the amount of observed squeezing [38]. With this information we can plan for permanent implementation of squeezing in advanced gravitational wave detectors.

Making informed assumptions about the improvements possible, we believe that it will be possible to inject squeezing with 20 % total effective losses (including OPO escape efficiency, injection losses, and losses in the interferometer detection chain) and approximately 15 mrad rms squeezing angle fluctuations in Advanced LIGO, making 6 dB of shot noise reduction possible. Frequency independent squeezing may provide a faster, simpler route towards good sensitivity than high power operation. At the full input power squeezing could be used to improve the signal to noise ratio for high frequency signals, such as binary coalescences. Once Advanced LIGO operates at its design sensitivity, a filter cavity will be needed to realize the full potential of squeezing by reducing the amount of squeezing injected at low frequencies [41].

12 Towards the quantum limit: an update from the AEI 10 m prototype (Presenter: T. Fricke)

The AEI 10 m prototype [17], currently under construction, is a Fabry-Perot Michelson interferometer designed to reach the standard quantum limit at a frequency of 200 Hz, allowing subsequent investigations into techniques to beat the SQL.

To increase the magnitude of quantum radiation pressure noise, low mass (100 g) mirrors are used to form the interferometer arm cavities. Each of these mirrors will be suspended by a triple pendulum, with a monolithic fused-silica final stage. Seismic isolation is provided by a soft passive plant based on inverted pendula and geometric anti-springs, enhanced through active feedback and feed-forward [19]. To further reduce relative motion, the seismic isolation tables are connected via a "suspension platform interferometer" [18] which measures and, via feedback, reduces the inter-table motion using interferometry.

One of the most challenging noise sources encountered by this experiment will be coating thermal noise, which motivates the use of large beam spots, and, consequently, marginally stable cavities. Our optical design features "tunable stability," allowing us

to start with shorter arm cavities and proceed stepwise towards longer arms with lower thermal noise [20].

The 10 meter prototype facility will provide a versatile test-bed for valuable experiments to be conducted while the big interferometers are busy collecting astrophysical observations.

13 Parametric instability (Presenter: C. Blair)

Parametric instability is one of the unsolved potential problems of advanced gravitational wave detectors. Results were presented on measurements of optically excited mechanical modes; from these results the parametric gain and the spatial overlap factor can be calculated as $(3.8 \pm 0.5) \times 10^3$ and 0.21 ± 0.04 respectively. These measurements are taken in a low power regime far from instability. This leads naturally to the proposition that such a procedure could be used for low power charaterisation of a cavity or complex system of cavities for their susceptibility to parametric instabilities. For more details see [21].

14 Mode healing in GW interferometers (Presenter: C. Bond)

For the commissioning of advanced detectors it is crucial to understand the behaviour of the interferometers in the presence of deviation of the mirror surfaces from an ideal sphere. This can result in distorted beams at the interferometer output. The presence of a signal recycling mirror (SRM), intended to enhance gravitational wave sidebands in the detector, has the additional benefit of healing the distorted beam. Observed in GEO600, it results from the effective cavity formed between the two interferometer arms and the SRM, in which the TEM_{00} mode is enhanced and higher-order spatial modes are suppressed.

Using the simulation program FINESSE [3] an initial investigation of this phenomenon was carried out for Advanced LIGO in the presence of unbalanced thermal distortions. The higher-order mode content at the dark port was observed to be strongly suppressed for increased SRM reflectivity with the signal recycling cavity tuned to the carrier. Further investigations are ongoing into the effect at different tunings of the SRM.

15 Mode-matching and astigmatism requirements for the use of higher-order LG mode beams in aLIGO (Presenter: B. Sorazu)

Next generation interferometric gravitation wave (GW) detectors are expected to be limited at peak sensitivity by coating thermal noise. Higher-order Laguerre-Gauss (LG) beams with a more homogeneously distributed intensity profile than the $LG_{0,0}$ mode is expected to reduce this thermal noise by a factor of 1.7 in amplitude spectral density. We have found that higher-order LG mode beams are more susceptible to astigmatism and mode mismatch than a $LG_{0,0}$ mode [22]. We used FINESSE to simulate two alternative aLIGO cavities [23,24] with round-trip diffraction losses of an

$LG_{3,3}$ beam that are equivalent to an $LG_{0,0}$ beam in standard aLIGO. The astigmatism tolerance for 1 % intracavity power loss is respectively 0.23 nm and 0.34 nm for the Zernike polynomial $Z_{2,2}$—similar to current metrology limits. The mode-matching tolerances are about 30 m in waist location and 0.3 mm in waist size.

16 Results from Raman spectroscopy and direct thermal noise measurements on tantala and silica coatings (Presenter: M. Granata)

In order to isolate the mechanisms behind thermal-noise fluctuations in optical coatings, the Laboratoire des Matériaux Avancés has started a collaboration with the Institut Lumière Matière to investigate the Raman spectra of ion-beam sputtered tantala samples with different annealing history. Work is presently ongoing to understand the observed behaviours, in order to correlate the mechanical loss to the evolutions of the Raman spectra. The same analysis will be shortly carried out on fused silica coatings too.

A novel technique of direct thermal noise measurements [25], developed by the École Normale Suprieure de Lyon, is presented. Measured samples are tipless cantilevers with ion-beam sputtered coatings of tantala or fused silica, annealed before and after the coating. In all cases, the power spectral density of the measured noise is inversely proportional to the frequency, as predicted by the structural noise model with constant loss.

17 Electro-optic modulators and power control for advanced LIGO (Presenter: D.B. Tanner for the IO group)

The Input Optics (IO) of Advanced LIGO includes custom-designed electro-optic modulators and laser power control. The phase modulators have 3 sets of RF electrodes in order to provide three modulation frequencies (9.1, 24.1, and 45.5 MHz) using a single RTP crystal. The crystal is slightly wedged to refract the wrong polarization by different angles than the desired one, sending the wrong one to a baffle and thereby reducing RF amplitude noise. RFAM is below 1×10^{-4} even with modulation depths approaching 0.4. The power control uses two thin-film polarizers, a water-cooled beam dump, and motorized half-wave plate allowing automated control of the laser power delivered to the input mode cleaner over a few mW to greater than 180 W. These devices met the requirements for Advanced LIGO.

18 Characterization of the LASY-50 CO_2 laser to be used in the advanced Virgo thermal compensation system (Presenter: E. Cesarini)

In second generation GW interferometric detectors optical aberrations in the recycling cavities need to be compensated using CO_2 projectors; the light at 10.6 μm is completely absorbed by the optics, providing focusing [26]. The AdV Virgo thermal compensation system employs the LASY-50 from Access Laser Company. An investigation of optical parameters ($w_0 = 0.98 \pm 0.01$ mm), gaussianity ($M^2 = 1.04$)

and astigmatism ($\epsilon = 0.93$) has been performed. A detailed study of the intensity noise of the laser has been done and an intensity stabilization system, to make the noise compliant with the AdV Virgo sensitivity. In addition, the DC pointing stability ($\theta_{MAX} = 0.15$ mrad) and the jitter noise spectrum have been measured.

19 Thermal compensation system for non-symmetric optical distortions in future gravitational wave detectors (Presenter: M. Lorenzini)

In second generation GW interferometric detectors, optical aberrations have both an axisymmetric and a non-symmetric contribution. The Advanced Virgo Thermal Compensation System (TCS) compensates for non-symmetric contributions with a Scanning System (SS) [27] for residual distortions; it scans the central area of a compensation plate with a CO_2 laser spot with adjustable intensity, making a heating pattern complementing the non-symmetric optical path distortions. The distorted optical path is sensed by wavefront detectors (Hartmann sensors); the map of the optimal heating pattern is obtained by an FEM analysis. A test setup was built using a CO_2 laser beam, driven by a pair of galvonometer mirrors and intensity modulated by an AOM. The RMS difference among the obtained and optimal pattern was $\sim 2\%$.

20 Automatic alignment for the GEO 600 squeezed light application (Presenter: E. Schreiber)

An important aspect of achieving the best possible performance for the GEO 600 squeezed light application [15] is a good alignment of the squeezed vacuum field to the carrier beam at the output of the Michelson interferometer. To ensure optimal alignment on long time scales and in the presence of suspended optics we have implemented an automatic alignment scheme. Differential wavefront sensing with sidebands of both the squeezed light field and the interferometer beam creates a relative alignment error signal. A piezo-driven steering mirror then actively optimizes the alignment. Stable control with a unity-gain frequency of up to 10 Hz was achieved and is especially successful in compensating long-term drifts, assuring a constant squeezing level.

21 Acoustic mode damper for parametric instabilities control (Presenter: S.Gras)

In the next few years as the advanced detectors are commissioned at high optical power, parametric instability (a three mode scattering process which can transfer optical energy into test mass acoustic vibrations; see [29–31]) becomes likely. The research focuses on the design and construction of piezoelectric resonant dampers for suppressing ultrasonic acoustic modes while avoiding a noise penalty. The prototype of a resonant damper demonstrated suppression of acoustic modes to be as high as three orders of magnitude. Our numerical analysis predicts a low thermal noise penalty, equivalent to 1–2 % degradation of the Advanced LIGO strain sensitivity. Such acoustic mode damper could be easily implemented in the detectors.

22 Characterization of the mirror internal losses of the suspended test masses by means of an interferometric sensor: results on the Virgo+ payloads and perspectives. (Presenter: V. Mangano on behalf of the Virgo Collaboration)

We have developed an interferometric sensor to characterize the internal losses of suspended mirrors. The system was developed by Naples group and installed in the Virgo Rome laboratory. The sensitivity requirements are based on the mirror quality factors (10^5 up to 10^7) with maximum decay amplitudes of the order of 10^{-10} m. A Michelson interferometer is placed in front of the suspended optical element to be measured. Two output ports are used to build a differential signal, which is also employed in the closed loop control system of the interferometer. The measurement of the mechanical quality factor Q is carried on with a standard ring-down technique.

This system was successfully tested on the mirrors dismounted from the Virgo+ interferometer, which have modal frequencies and Qs are similar to the ones measured in Advanced Virgo. The developed device can be a good and reliable sensor for characterizing the mechanical losses of the mirrors before installing them in the gravitational wave detector.

23 A solution of an offset problem in detuned RSE (Presenter: N. Saito)

In order to surpass the standard quantum limit, we can make an optical spring and increase a signal around its resonant frequency by detuning a signal recycling mirror. There is a problem, however, that an offset on the control signal obtained by a PM sideband decreases the photo-detector resolution by the detuning. We propose to use an additional AM sideband to cancel the offset at the control signal extraction port. We verified the method by a simulation and performed a proof-of-principle experiment.

24 The AEI 10 m prototype interferometer frequency control using a reference cavity (Presenter: F. Kawazoe for the AEI 10 m Prototype team)

The AEI 10 m Prototype project will provide a test bed for a sub-SQL interferometer. Success requires all possible noise sources to be suppressed sufficiently including laser frequency noise. An NPRO 2 W Nd:YAG laser frequency will be stabilized to a level of 10^{-4} Hz/$\sqrt{\text{Hz}}$ at 20 Hz rolling off to below 6×10^{-6} Hz/$\sqrt{\text{Hz}}$ above 1 kHz, with the safety margin of 10, by using a 20 m length triangular suspended cavity. In addition, an angular control system will be used to reach this stringent requirement whose degrees of freedom are introduced in [32].

25 Design of a glass optical parametric oscillator to produce audio frequency squeezing for gravitational wave detection (Presenter: G. Mansell)

The next generation of interferometric gravitational-wave detectors will probably employ squeezed states of light to increase their sensitivity. The squeezed light source

must operate at low frequencies, be vacuum compatible, and produce squeezing over long time scales. The design of a glass optical parametric oscillator (OPO) cavity, which is expected to produce greater than 10 dB squeezing in the audio frequency band, was presented. The glass-based design is chosen for its long term stability and vacuum compatibility. The cavity will be in a bow-tie configuration for backscatter resistance [33], and doubly resonant at the 532 nm pump and 1,064 nm fundamental wavelengths. Components will be mounted on a glass slab base using the optical contacting technique. Design challenges such as the mounting of the nonlinear crystal, alignment tolerances, phase matching and temperature control were addressed.

26 Active thermal lensing elements for spherical and astigmatic mode matching (Presenter: P. Fulda)

We report on the development of a thermally driven actuator for correcting circular and astigmatic mode mismatches. The maximum range required from such a device in order to maintain mode matching in the aLIGO input optics path is expected to be around -130 mD of focal power (focal length of ~ -8 m), in the complete absence of any core optics thermal compensation. With the inclusion of the already developed ring heater and CO_2 laser thermal compensation however, the reported device will be required to produce only a fraction of this dynamic range.

In-air tests of an initial prototype have shown a dynamic range of up to -100 mD focal power [34]. Use of the actuator in a beam-shape feedback control loop was also demonstrated [35]. An advanced prototype has recently been tested in vacuum, with a demonstrated dynamic range up to -50 mD focal power. Diagnostic cavity scan measurements of higher-order mode spectra in transmission of the actuator have shown no degradation in transmitted mode purity associated with actuation of the device. By contrast the actuator was demonstrated to increase the mode purity by correcting for astigmatism already present in the incident beam.
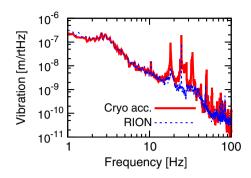
27 Development of a cryogenic accelerometer for the Japanese GW observatory KAGRA (Presenter: D. Chen)

The 4 main mirrors of the KAGRA interferometer are planned to be cooled to 20 K. Radiation shield vibration can couple into the detector signal via scattered light. In order to measure the shield vibration at low temperature for investigating the impact on the KAGRA sensitivity, we developed a Michelson interferometer-based accelerometer operating at cryogenic temperature.

The accelerometer was characterized when cooled to 28 K using a test cryostat. A coincidence measurement with a commercial RION accelerometer placed outside the cryostat has proved that the two signals are consistent with each other. Thus, the developed accelerometer can be employed to analyze the radiation shield vibration in the real KAGRA cryostats (Fig. 5).

Fig. 5 Test of the Kagra
Cryogenic Accelerometer.
(T = 28 K)

28 Design study of the KAGRA OMC (Presenter: A. Kumeta)

For KAGRA, the output mode cleaner (OMC) plays an important role in filtering out unnecessary light that could impose excess quantum noise. We present an optimized design, using the FINESSE simulation code, of the OMC to realize the target sensitivity of KAGRA. We use a realistic mirror map and consider the spatial modes up to the 10th order. We have found that the target sensitivity can be achieved using a 4-mirror OMC with a roundtrip length of 174 cm, a Gouy phase shift of 38°, and a finesse of 780.

29 Impact of backscattered-light in squeezing-enhanced LIGO (Presenter: L. Barsotti for the team)

To establish the use of squeezed light as a realistic option for the next generation of detectors, we studied and quantified relevant noise coupling mechanisms through a direct measurement of the impact of backscattered-light from a squeezed-light source on one of the LIGO 4 km long detectors. This backscattered-light power was determined to be 260 fW, and the noise level was at least a factor of 5 below the interferometer quantum noise in the 50–300 Hz detection region. We showed how our measurements compare to backscattering requirements for advanced detectors currently under construction, such as Advanced LIGO, and how it informs the design of compatible squeezed light sources. For more details see [37].

30 A new set up for torsion-bar antenna (Presenter: A. Shoda)

We are constructing a gravitational wave detector called Phase-II Torsion-bar Antenna (TOBA), which uses the rotation of test mass bars to sense the tidal force of gravitational waves. TOBA can achieve a good sensitivity even on the ground at low frequencies, with the target sensitivity of the Phase-II TOBA being 10^{-15} [$1/\sqrt{Hz}$] at 1 Hz. It features the use of two test masses with a suspended optical bench for common mode noise rejection, cryogenic operation for thermal noise reduction and an active vibration isolation stage for further noise suppression. In addition, its detection volume and angular resolution can be improved by simultaneously monitoring the vertical and horizontal rotations of the test masses. Phase-II TOBA will be used for addressing

technical issues for 10-m scaled future detectors [28] as well as conducting collaborative research with other detectors such as the development of cryogenic systems or Newtonian noise studies.

31 Temperature effects on the optical properties of highly uniform, porous, amorphous Ta$_2$O$_5$ coatings on silica (Presenter: G. Gemme)

We present spectroscopic ellipsometry results (0.755 eV range) obtained on Ta$_2$O$_5$ coatings deposited on silica substrates by ion sputtering. Two sets of samples of different thickness were considered: a sub-set was treated with post-growth annealing, in different conditions. Absorption losses data were obtained with photothermal common-path interferometry at 1,064 nm. The best simulation of data was obtained using the CodyLorentz approach on a three-phase model (substrate/film/surface) and a quasi-uniform density ($\sim 7\%$) of empty spherical pores inside the coating. The analysis of samples annealed to increasingly higher temperatures showed a slight blue-shift of the energy gap, an increase in the pore volume fraction, an increase ($\sim 1\%$) in the coating thickness, a small ($< 1\%$) reduction in the index of refraction in the transparency region and a limited increase in absorption losses. These findings were interpreted [40] in terms of a release of the compressive strain inherent to the deposition process.

32 Finite element simulations of electromagnetic effects in the advanced Virgo payload assembly (Presenter: G. Gemme)

For Advanced VIRGO, the electromagnetic interaction among the different parts of the payload (the mechanical structure holding and positioning the mirrors) has undesirable side-effects identified in the dissipation mechanisms due to eddy currents, signal cross-talk among driving coils and magnet misalignment. We have undertaken a series of finite element electromagnetic computations involving significant parts of the payload: the coil disk/marionette and the mirror/cage assemblies. After validating the algorithms on analytical test cases, we have addressed 4 items: (a) the effect of magnet misalignment, (b) the power dissipation due to the eddy currents caused by the moving magnets in the mirror/cage subsystem, (c) the signal cross-talk among driving coils and their power dissipation and (d) the direct coupling of the magnets to an external field.

33 In situ correction of mirror surface defects for second and third generation gravitational wave detectors (Presenter: G. Vajente)

The sensitivity of interferometric gravitational wave detectors depends crucially on the mirror quality [42]. The requirements on the mirror surface roughness at various spatial frequency are very stringent and in many cases beyond the present metrology and polishing capabilities.

We describe an in-situ correction system based on the projection of a thermal pattern on the high reflectivity surface of the mirrors [43]. In this way it is possible to correct for defects at low and medium spatial frequency, allowing a reduction of the round

trip losses and an improvement of the final sensitivity. In the case of third generation detector, using the proposed technique it is possible to correct the surface defects that will otherwise prevent the use of high order Laguerre-Gauss modes, opening the possibility of a significant improvement of the thermal noise limited sensitivity.

34 Squeezed quadrature fluctuations in a gravitational wave interferometer (Presenter: S. Dwyer)

The level of quantum noise reduction achieved through squeezing injection is limited by optical losses and by the fluctuations of the quadrature angle of the injected squeezing. In order to achieve the high levels of squeezing (10 dB) desired for third generation interferometers, the squeezing angle fluctuations must be reduced to less than 10 mrad. We have calculated the effect of experimental realities such as fluctuations of the length of the optical parametric oscillator (OPO) and the temperature of the nonlinear crystal on the squeezing angle. We also understood an unanticipated coupling of relative alignment fluctuations between the squeezed beam and the interferometer beam to the squeezing angle, which accounted for most of the 35 mrad rms squeezing angle fluctuations observed durring the LIGO squeezing expiriment. A modification to the control scheme and reduction of the OPO length noise should reduce the squeezed quadrature fluctuations to 5–10 mrad, an acceptable level for Advanced LIGO and third generation interferometers [38].

35 Stray light control in KAGRA (Presenter: T. Akutsu)

As for all the advanced interferometers, KAGRA's output may be disturbed by stray light. Our requirement is that the equivalent displacement noise due to the stray light be suppressed to less than 1/100 of the goal sensitivity of KAGRA. For this purpose, five kinds of baffles and beam damps will be installed: (1) arm duct baffles, (2) cryoduct shields, (3) narrow-angle baffles, (4) wide-angle baffles, (5) others. They are all installed in the ultra high vacuum, 10^{-7} Pa. In addition, (2) and (4) will be cooled down to 20 and 80 K respectively, because they are installed in the cryostats.

The planned surface finish survived several tests; it is compatible with the environment, and has a low reflectivity of a few per cent; the scattering distribution for the laser light is also low. The manufacturing of the baffles has started.

This work is supported by Advanced Technology Center of National Astronomical Observatory of Japan (NAOJ). JASMINE project office in NAOJ helped us use their scatterometer. Mike Smith (LIGO) helped us make an initial conceptual design of stray-light control of KAGRA.

36 Obtaining the deformation noise spectral density for the Schenberg detector using FEM (Presenter: F. S. Bortoli)

Schenberg is a spherical resonant mass gravitational wave detector. Its center operation frequency is 3,200 Hz. Transducers [39] located on the surface of resonant sphere,

following a half dodecahedron distribution, are used to monitor the sphere surface displacement amplitude. The development of mechanical impedance matchers for coupling the transducers to the sphere in the Mario Schenberg detector is challenging due, to a large extent, on its reduced size. We developed a design of the single-mode impedance matcher in which all the modes of the system sphere plus the impedance matcher had similar shapes and could be calibrated in the same way. We found that the vibration amplification is of the order of 100 (considering the length) and the bandwidth is of the order of 30 Hz which is one hundredth of the operational frequency (the inverse of the amplification factor), very much as it is predicted by theory using the "lumped" model. Thus, the FEM simulation presented the same results predicted by the theory.

37 Optomechanical characterization of silicon nitride membranes (Presenter: M. Leonardi)

The sensitivity of the next generation of Earth based gravitational wave detector will be limited in the middle range of frequency by the brownian noise of the coating. In particular, the critical material is the tantalum oxide (Ta_2O_5). We investigated an alternative material, silicon nitride (SiN), in particular SiN membranes. By investigating the loss angle of the modes of the membranes as a function of the internal stress, we were able to measure the loss angle of the SiN material and to verify quantitatively the dependence of the loss angle from the internal stress of the membrane. The resulting loss angle of SiN is 9.0×10^{-5} with a 5 % uncertainty. We extended the investigation to the optical losses of the SiN membranes at 1,064 nm using a Fabry-Perot cavity with the membrane in the middle.

38 Parametric instability in KAGRA (Presenter: K. Shibata)

Parametric instability (PI) happens when higher order modes generated by optical-mechanical scattering resonate in a cavity. This process can cause a lock loss of an interferometer. Therefore, we need to estimate the risk of the PI to design a gravitational wave detector. We derived a general condition for the generation of the PI which is applicable to arbitrary optical configurations. When applied to KAGRA, the risk of the PI (parametric gain) predicted by this new method is several times lower than the previous estimates, where the Gouy phase shifts in the recycling cavities had been ignored. This is because Gouy phase shifts in the recycling cavities prevent the power build up of higher order modes in most cases. Still, depending on the radius of the curvature of the actually delivered mirrors, there are a few potential PI modes in KAGRA which have to be properly damped by active feedback to the mirror actuators, if these modes are excited.

39 Optical setup and auto alignment for the frequency reference cavity at the AEI 10 m Prototype interferometer (Presenter: M. Hanke)

One ambitious goal for the 10 m Prototype facility currently being set up at the AEI Hannover is to reach and subsequently even surpass the standard quantum limit in a detection band around 200 Hz with a 10 m arm length Michelson interferometer. In order to pursue such an avenue, the laser source must be extremely well stabilised and highly reliable. The laser source is a AEI-LZH 35 W Nd:YAG laser also used to drive the km-scale gravitational wave observatories, LIGO and GEO 600. A 23 m long fully suspended triangular ring cavity of finesse ca. 3,000 will be used as a frequency reference for the stabilisation of the laser. The aim of this project, the frequency reference cavity, is to reach a level of laser frequency fluctuations of better than $10^{-5}/\sqrt{\text{Hz}}$ in the detection band, centered around 200 Hz. Therefore we need to reduce the frequency noise of the free running laser by a factor of a million.

References

1. Aasi, J. et al.: arXiv:1304.0670 (2013)
2. Accadia, T., et al.: The virgo collaboration. JINST **7**, P03012 (2012)
3. Freise, A., Heinzel, G., Lück, H., Schilling, R., Willke, B., Danzmann, K. Class. Quantum Gravity **21**, S1067, the program is http://www.gwoptics.org/finesse (2004)
4. Fafone, V., et al.: Virgo note 0677E–09
5. Blom, M.R., et al.: Nucl. Instrum. Methods Phys. Res. A **718**, 466–470 (2013)
6. Winkelmann, L., et al.: Appl. Phys. B Lasers Opt. **102**(3), 529–538 (2011)
7. Kwee, P., et al.: Opt. Express **20**(10), 10617–10634 (2012)
8. Kwee, P., et al.: Opt. Lett. **36**(18), 3563–3565 (2011)
9. Kwee, P., et al.: Rev. Sci. Instrum. **78**, 073103 (2007)
10. Meier, T., et al.: Opt. Lett. **35**(22), 3742–3744 (2010)
11. Carbone, L., et al.: Phys. Rev. Lett. **110**, 251101 (2013)
12. Theeg, T., et al.: IEEE Photonics Technol. Lett. **24**(20), 1864–1867 (2012)
13. Was, M., et al.: A fixed false alarm probability figure of merit for gravitational wave detectors, in preparation
14. Lück, H., et al.: J. Phys. Conf. Ser. **228**, 012012+ (2010)
15. Grote, H., et al.: Phys. Rev. Lett. **110**, 181101+ (2013)
16. Wittel, H., et al.: Thermal Correction of Astigmatism in the Gravitational Wave Observatory GEO 600, in preparation
17. Westphal, T., et al.: Appl. Phys. B. **106**(3), 551–557 (2012)
18. Dahl, K., et al.: Class. Quantum Gravity **29**, 095024 (2012)
19. Wanner, A., et al.: Class. Quantum Gravity **29**, 245007 (2012)
20. Gräf, C., et al.: Class. Quantum Gravity **29**, 075003 (2012)
21. Blair, C., Susmithan, S., Zhao, C., Fang, Q., Ju, L., Blair, D.: Phys. Lett. A **377**(31–33), 1970–1973 (2013). doi:10.1016/j.physleta.2013.05.019
22. Sorazu, B., et al.: Class. Quantum Gravity **30**, 035004 (2013)
23. Bond, C., Fulda, P., Carbone, L., Kokeyama, K., Freise, A.: Phys. Rev. D **84**, 102002 (2011)
24. Hong, T., Miller, J., Yamamoto, H., Chen, Y., Adhikari, R.: Phys. Rev. D **84**, 102001 (2011)
25. Bellon, L., Ciliberto, S., Boubaker, H., Guyon, L.: Opt. Commun. **207**, 49–56 (2002)
26. Rocchi, A., et al.: J.P.C.S. **363**, 012016 (2012)
27. Lawrence, R.C.: Active Wavefront Correction in Laser Interferometric Gravitational Waves Detectors, PhD thesis, MIT (2003)
28. Ando, M., et al.: Phys. Rev. Lett. **105**(16), 161101 (2010)
29. Braginsky, V.B., Strigin, S.E., Vyatchanin, S.P.: Phys. Lett. A **287**(56), 3 (2001)
30. Evans, M., Barsotti, L., Fritschel, P.: Phys. Lett. A **374**, 4 (2010)

31. Zhao, C., Ju, L., Fan, Y., Gras, S., Slagmolen, B.J.J., Miao, H., Barriga, P., Blair, D.G.: Phys. Rev. A **78**, 2 (2008)
32. Kawazoe, F., Schilling, R., Lück, H.: J. Opt. **13**, 055504 (2011)
33. Chua, S.S.Y., et al.: Opt. Lett. **36**(23), 4680 (2011)
34. Arain, M., et al.: Opt. Express **18**, 2767 (2010)
35. Liu, Z., et al.: Appl. Opt. **26**(52), 6452 (2013)
36. Aasi, J., et al.: Nat. Photon **7**, 613–619 (2013)
37. Chua, S.S.Y., et al.: Preprint arXiv:1307.8176v2 (2013)
38. Dwyer, S., et al.: Opt. Express **16**, 19047–19060 (2013)
39. Frajuca, C., et al.: CQG **7**, 1961 (2002)
40. Anghinolfi, L.: J. Phys. D Appl. Phys. **46**, 455301 (2013)
41. Evans, M., Barsotti, L., Kwee, P., Harms, J., Miao, H.: Phys. Rev. D **88**, 022002 (2013)
42. Day, R.A., Vajente, G., Kasprzack, M., Marque, J.: Phys. Rev. D **87**, 082003 (2013)
43. Vajente, G., Day, R.A.: Phys. Rev. D **87**, 122005 (2013)

Author affiliations

M. Adier · G. Cagnoli · J. Degallaix · V. Dolique · R. Flaminio · D. Forest · M. Granata · B. Lagrange ·
C. Michel · L. Pinard · P. Risson · B. Sassolas · N. Straniero
Laboratoire des Matériaux Avancés (CNRS/IN2P3), Université de Lyon, Villeurbanne, Lyon, France

F. Aguilar · L. Bellon · M. Geitner · T. Li
Ecole Normale Supérieure, 46 allée d'Italie, 69007 Lyon, France

T. Akutsu · D. Friedrich · R. Takahashi · Y. Niwa
National Astronomical Observatory, 2-21-1 Osawa, Mitaka-shi, Tokyo, Japan

M. A. Arain · G. Ciani · D. Feldbaum · P. Fulda · J. Gleason · M. Heintze · Z. Liu · R. Martin · C. L. Mueller ·
G. Mueller · D. Nanda Kumar · V. Quetschke · D. H. Reitze · D. B. Tanner · G. Tellez · L. Williams
University of Florida, Gainesville, FL, USA

M. Ando · Y. Aso · K. Okada · K. Shibata · A. Shoda · K. Tsubono
Department of Physics, University of Tokyo, Tokyo, Japan

L. Anghinolfi
Laboratory for Micro and Nanotechnology, Paul Scherrer Institute, Villigen, Switzerland

L. Anghinolfi · M. Canepa
Universit degli Studi di Genova, 16146 Genova, Italy

P. Antonini
Centro Ricerche E.Fermi, Roma, Italy

B. W. Barr · A. S. Bell · C. Bond · L. Carbone · A. Freise · P. Fulda · N. Gordon · C. Gräf · S. Hild ·
S. H. Huttner · S. Leavey · J. Macarthur · B. Sorazu · K. A. Strain
SUPA School of Physics and Astronomy, University of Glasgow, G12 8QQ Glasgow, Scotland, UK

L. Barsotti · S. Dwyer · M. Evans · P. Fritschel · S. Gras · N. Mavalvala · N. Smith-Lefebvre
Massachusetts Institute of Technology, NW 22-295, 185 Albany Street, Cambridge, MA, USA

M. G. Beker · A. Bertolini · M. R. Blom · H. J. Bulten · M. Doets · E. Hennes · F. Mul · A. Schimmel ·
J. F. J. van den Brand
Nikhef Amsterdam, Science Park 105, 1098 XG Amsterdam, The Netherlands

C. Blair
M013 University of Western Australia, Nedlands, WA 6009, Australia

C. Bogan · T. Fricke · S. Goßler · M. Hanke · A. Khalaidovski · P. Kwee · T. Meier · P. Oppermann ·
J. Poeld · R. Schnabel · B. Willke
Albert-Einstein-Institut, Max-Planck-Institut fuer Gravitationsphysik and Leibniz Universität Hannover,
Hannover, Germany

C. Bond · D. Brown · L. Carbone · A. Freise
School of Physics and Astronomy, University of Birmingham, Birmingham, UK

F. S. Bortoli · C. Frajuca
IFSP, Sao Paulo, Brazil

B. C. Buchler · S. S. Y. Chua · P. K. Lam · C. M. Mow-Lowry · G. Mansell · D. E. McClelland ·
D. A. Shaddock · M. S. Stefszky · A. Wade · R. Ward
Department of Quantum Science, The Australian National University, Acton, ACT 0200, Australia

H. J. Bulten · J. F. J. van den Brand
VU University Amsterdam, De Boelelaan 1081, 1081 HVAmsterdam, The Netherlands

M. Canepa
Consorzio Interuniversitario per le Scienze Fisiche della Materia (CNISM), Sezione di Genova,
16146 Genova, Italy

M. Canepa · A. Chincarini · S. Farinon · G. Gemme · M. Neri · M. Prato
Istituto Nazionale di Fisica Nucleare (INFN), Sezione di Genova, 16146 Genova, Italy

E. Cesarini · E. Coccia · M. Cortese · V. Fafone · M. Lorenzini · D. Lumaca · V. Malvezzi · Y. Minenkov ·
L. Mudadu · I. Nardecchia · A. Rocchi · V. Sequino
INFN Roma Tor Vergata, via della Ricerca Scientifica 1, 00133 Roma, Italy

B. Champagnon · D. De Ligny · A. Mermet
Institut Lumière Matière, 10 rue Ada Byron, 69100 Villeurbanne, France

D. Chen · S. Kawamura · A. Khalaidovski · K. Kuroda · M. Ohashi · Y. Sakakibara · C. Tokoku ·
T. Uchiyama · K. Yamamoto
Institute for Cosmic Ray Research (ICRR), The University of Tokyo, Chiba, Japan

A. Chtanov · M. Gross
CSIRO Division of Materials Science and Engineering, PO Box 218, Lindfield, NSW 2070, Australia

A. Conte · E. Majorana · L. Naticchioni
Universit di Roma "La Sapienza", 00185 Roma, Italy

A. Conte · E. Majorana · P. Puppo
Istituto Nazionale di Fisica Nucleare (INFN), Sezione di Roma, 00185 Roma, Italy

M. Daloisio
Padova University, Padova, Italy

M. Daloisio · J.-P. Zendri
INFN, 35131 Padova, Italy

M. Damjanic · O. Puncken · T. Theeg · P. Wessels · L. Winkelmann
Laser Zentrum Hannover e.V., Hannover, Germany

R. A. Day · M. Kasprzack · J. Marque
European Gravitational Observatory, Cascina, Italy

K. Dooley · H. Grote · F. Kawazoe · E. Schreiber · H. Vahlbruch
Albert-Einstein-Institut, Max-Planck-Institut fuer Gravitationsphysik, Callinstr. 38,
30167 Hannover, Germany

M. Factourovich
Columbia University, New York, NY 10027, USA

M. Frede
neoLASE GmbH, Hannover, Germany

V. V. Frolov · D. Martynov
LIGO Livingston Observatory, PO Box 940, Livingston, LA 70754, USA

R. Gustafson · G. D. Meadors
University of Michigan, Ann Arbor, MI 48109, USA

K. Ishidoshiro
Tohoku University, Sendai, Japan

D. Sigg · K. Izumi · K. Kawabe · M. Landry · C. Vorvick
LIGO Hanford Observatory, PO Box 159, Richland, WA 99352, USA

M. Kasprzack
Laboratoire de l'Accélérateur Linéaire, Orsay, France

N. Kimura · S. Koike · T. Kume · Y. Saito · T. Suzuki
High Energy Accelerator Research Organization (KEK), Tsukuba, Japan

A. Kumeta · K. Somiya · S. Ueda
Tokyo Institute of Technology, Tokyo, Japan

M. Leonardi · G. A. Prodi
Trento University and INFN, 38123 Povo, Trento, Italy

Z. Liu
School of Applied and Engineering Physics, Cornell University, Ithaca, NY, USA

G. Losurdo
Istituto Nazionale di Fisica Nucleare, Sez. di Firenze - Via G. Sansone 1, 50019 - Sesto F., Firenze, Italy

N. S. Magalhaes
UNIFESP, Sao Paulo, Brazil

V. Mangano
INFN, Roma, Italy

M. Neri
Universit degli Studi di Genova, 16146 Genova, Italy

M. Prato
Nanochemistry, Istituto Italiano di Tecnologia (IIT), 16163 Roma, Italy

V. Quetschke
The University of Texas at Brownsville, Brownsville, TX 78520, USA

N. Saito
Graduate School of Humanities and Sciences, Ochanomizu University, 2-1-1 Otsuka, Bunkyo-ku, Tokyo, Japan

R. M. S. Schofield
University of Oregon, Eugene, OR 97403, USA

E. Serra
IFN CNR-FBK and INFN, 38123 Povo, Trento, Italy

G. Vajente
Istituto Nazionale di Fisica Nucleare, Sez. di Firenze - Largo B. Pontecorvo 3, 56127 Pisa, Italy